CrossMark

RESEARCH PAPER

Analysis of fucosylation in liver-secreted N-glycoproteins from human hepatocellular carcinoma plasma using liquid chromatography with tandem mass spectrometry

Eun Sun Ji[1] · Heeyoun Hwang[1] · Gun Wook Park[1,2] · Ju Yeon Lee[1] ·
Hyun Kyoung Lee[1,2] · Na Young Choi[1,2] · Hoi Keun Jeong[1,2] · Kwang Hoe Kim[1,2] ·
Jin Young Kim[1] · Seungho Lee[3] · Yeong Hee Ahn[4] · Jong Shin Yoo[1,2]

Abstract Fucosylation of N-glycoproteins has been implicated in various diseases, such as hepatocellular carcinoma (HCC). However, few studies have performed site-specific analysis of fucosylation in liver-secreted proteins. In this study, we characterized the fucosylation patterns of liver-secreted proteins in HCC plasma using a workflow to identify site-specific N-glycoproteins, where characteristic B- and/or Y-ion series with and without fucose in collision-induced dissociation were used in tandem mass spectrometry. In total, 71 fucosylated N-glycopeptides from 13 major liver-secreted proteins in human plasma were globally identified by LC-MS/MS. Additionally, 37 fucosylated N-glycopeptides were newly identified from nine liver-secreted proteins, including alpha-1-antichymotrypsin, alpha-1-antitrypsin, alpha-2-HS-glycoprotein, ceruloplasmin, alpha-1-acid glycoprotein 1/2, alpha-2-macroglobulin, serotransferrin, and beta-2-glycoprotein 1. Of the fucosylated N-glycopeptides, bi- and tri-antennary glycoforms were the most common ones identified in liver-secreted proteins from HCC plasma. Therefore, we suggest that this analytical method is effective for characterizing fucosylation in liver-secreted proteins.

Keywords N-Glycoproteins · Fucosylation · Liquid chromatography · Mass spectrometry · Human plasma · Liver-secreted glycoproteins

Eun Sun Ji and Heeyoun Hwang contributed equally to this work.

✉ Yeong Hee Ahn
  ahnyh@cju.ac.kr

✉ Jong Shin Yoo
  jongshin@kbsi.re.kr

[1] Biomedical Omics Group, Korea Basic Science Institute, 162 YeonGuDanji-Ro, Ochang-eup, Cheongju, Chungbuk 28119, Republic of Korea

[2] Graduate School of Analytical Science and Technology, Chungnam National University, Daejeon 305-764, Republic of Korea

[3] Department of Chemistry, Hannam University, Daejeon 306-791, Republic of Korea

[4] Department of Biomedical Science, Cheongju University, Cheongju 28503, Republic of Korea

Abbreviations

A2M	Alpha-2-macroglobulin
AACT	Alpha-1-antichymotrypsin
AAT	Alpha-1-antitrypsin
AGP1	Alpha-1-acid glycoprotein 1
AGP2	Alpha-1-acid glycoprotein 2
APOH	Beta-2-glycoprotein 1
CID	Collision-induced dissociation
CP	Ceruloplasmin
FETUA	Fetuin A
Fuc	Fucose
HCC	Hepatocellular carcinoma
HCD	Higher-energy collision dissociation
Hex	Hexose
HexNAc	N-Acetyl hexosamine
HILIC	Hydrophilic interaction liquid chromatography
HP	Haptoglobin
HPX	Hemopexin
KNG1	Kininogen-1
MS	Mass spectrometry
N	Asparagine

Sia	Sialic acid
TF	Serotransferrin
VTN	Vitronectin

Introduction

Protein glycosylation is involved in adhesion, metastasis, and signaling through cell–cell interactions. Glycosylation is divided into O-glycosylation and N-glycosylation based on binding groups (i.e., hydroxyl serine (S) or threonine (T) side chains and carboxyl-amido asparagine (N) residue side chains, respectively) [1]. N-Glycosylation, which is classified into three glycan types, high-mannose, hybrid, and complex [2], occurs at the consensus tri-peptide sequence NXS/T, where X can be any amino acid except proline, in the ER and Golgi apparatus [3]. Aberrant glycosylation of the complex type, including fucosylation by fucosyltransferases and additional branching by N-acetylglucosaminyltransferase V (GnTV), occurs in cancer cells and is involved in adhesion to other cells, invasion into the extracellular matrix, and metastasis [4]. The fucosylation of N-glycoproteins in hepatocellular carcinoma (HCC) tissue was reported to increase the transcript and protein levels of the fucosyltransferase genes Fut 6 and Fut 8, which are involved in glycan fucosylation [5–7].

Anderson and Anderson first reviewed 289 proteins with a dynamic range in concentrations of more than 10 orders of magnitude [8]; since then, a total of 1929 non-redundant proteins with a <1 % false discovery rate have been reported in the PeptideAtlas [9]. A number of these proteins are synthesized and secreted by the liver and function in hemostasis and fibrinolysis and as carriers of various small molecules, lipids, and hormones [10]. Additionally, most liver-enriched proteins were recently classified by the human protein atlas (HPA) project as secreted proteins using microarray-based immunohistochemistry [11]. Alpha feto-protein (AFP), a well-known HCC biomarker approved by the FDA, is synthesized in liver tissue and secreted into plasma [12]. In particular, fucosylated AFP (AFP-L3), an aberrant N-glycoprotein created via fucosylation that exhibits an increased affinity for the fucose-specific lectin Lens Culinaris Agglutinin (LCA), was reported as a better biomarker for HCC than AFP [13–17]. Fucosylated AFP is increased in human serum and plasma from patients with liver cancer [18, 19]. Aberrant glycoproteins in the blood stream may reflect abnormal states in patients with cancer and could be developed as serological cancer biomarkers [20–24].

Mass spectrometry (MS), a powerful technology in proteomic fields, can play a central role in identifying aberrant glycoproteins from various disease-related biological media. Recently, the use of high-resolution tandem MS combined with nano-LC led to identification of the site-specific N-glycopeptides of major proteins, such as haptoglobin (HP) and vitronectin (VTN), in human HCC plasma by the targeted protein enrichment method [25–28] as well as HILIC enrichment methods [29, 30]. The antibody method for the Lewis Y structure and glycan level analysis of purified glycoforms confirmed that the fucosylated glycan level of HP is increased in HCC plasma [26, 31, 32]. Tang and colleagues reported an automatic analysis and label-free quantification method, where several N-glycopeptides from four proteins (HP, VTN, complement C3 protein, and hemopexin) were found to be increased in HCC sera [33]. However, they had previously identified 103 N-glycopeptides from 33 serum proteins [34] and reported that only four fucosylated N-glycopeptides were increased in HCC sera [33]. This discrepancy led us to more closely examine the different types of fucosylated proteins from human HCC plasma.

In this study, we selected 13 liver-secreted proteins to identify fucosylated glycoproteins in HCC plasma. We identified N-glycopeptides and their fucosylated forms, which were analyzed in previous research [28, 35–38]. We report herein the analysis workflow for liver-secreted protein fucosylation in human HCC plasma using LC-MS/MS.

Materials and methods

Materials

K$_2$EDTA-treated human plasma from patients with HCC was prepared at Severance Medical Center, Yonsei University (Seoul, Korea), with the consent of the blood donors and in accordance with Institutional Review Board guidelines (Electronic Supplementary Material (ESM) Table S1); it was stored at −80 °C until use. A multiple affinity removal system (MARS) column was purchased from Agilent (Wilmington, DE, USA). For glycopeptide enrichment, a ZIC-HILIC kit (ProteoExtract Glycopeptide Enrichment Kit) was obtained from EMD Millipore (Billerica, MA). Trypsin (mass spectrometry grade) for protein digestion was obtained from Promega (Madison, WI). Additionally, 1,4-dithiothreitol (DTT), iodoacetamide (IAA), trifluoroacetic acid (TFA), and formic acid (FA) were purchased from Sigma-Aldrich (St. Louis, MO). HPLC-grade acetonitrile (ACN) was also purchased (J.T. Baker, Phillipsburg, NJ).

Methods

Digestion of depleted and non-depleted plasma proteins

A MARS (Agilent) with an HP1100LC system (Agilent) was used to deplete the six most abundant proteins (albumin, transferrin, Ig gamma chain C region (IgG), Ig alpha chain C region (IgA), HP, and alpha-1-antitrypsin (AAT)) in plasma collected from 10 patients with HCC. Based on the manufacturer's

instructions, the human plasma samples were diluted by a factor of five in buffer A, which contained protease inhibitors, before centrifuging through 0.22-μm filters. Diluted plasma samples were injected at a flow rate of 0.25 ml/min (0 % B buffer) for 9 min. The bound fractions were eluted with buffer B (100 %) at a flow rate of 1 ml/min for 3.5 min. The column was regenerated by equilibrating in buffer B (0 %) for 7.5 min. Flow-through fractions collected from MARS-depleted plasma were stored at −20 °C until use. A pooled plasma sample was prepared by mixing 10 MARS-depleted plasmas from the HCC samples. The pooled plasma sample was desalted and concentrated by centrifugal filtration using 10-kDa molecular weight cutoff (MWCO) VIVASPIN filters (Sartorius, Göttingen, Germany). The plasma protein concentrations were determined by Bradford protein assay after filtering for molecular weight. The pooled sample (100 μg) was reduced with 5 mM DTT, alkylated with 12.5 mM IAA, and digested with trypsin (the substrate/enzyme ratio of 10:1) overnight at 37 °C. The digested sample was dried in a SpeedVac for HILIC enrichment.

N-Glycopeptide enrichment by HILIC

N-Glycopeptide enrichment with a ZIC-HILIC kit (ProteoExtract Glycopeptide Enrichment Kit) was performed according to the manufacturer's instructions (EMD Millipore). This kit includes ZIC Glycocapture Resin, ZIC Binding Buffer, ZIC Wash Buffer, and ZIC Elution Buffer. Briefly, 10 μl plasma digests (3 μg/μl concentration) was prepared by adding 50 μl ZIC Binding Buffer mixed with 50 μl homogenous ZIC Glycocapture Resin by pipetting up and down and incubated for 20 min. The incubated resin was then transferred to a new 1.5-ml tube and centrifuged (2 min, 250×g). The supernatant was discarded. The centrifuged resin was washed three times with 150 μl ZIC Wash Buffer. After adding 75 μl ZIC Elution Buffer for N-glycopeptide elution, the tube was incubated for 5 min with agitation and centrifuged for 2 min at 2500×g. The supernatant, containing the N-glycopeptides, was transferred to a new 1.5-ml tube and centrifuged for 2 min at 10,000×g. The N-glycopeptide supernatant was transferred to a new 1.5-ml tube, avoiding the transfer of resin particles. For LC/MSMS analysis, the HILIC-enriched peptide solution from plasma was dried in a SpeedVac and reconstituted in 100 μl 0.1 % FA/99.95 % ddH$_2$O.

Analysis using nano-liquid chromatography/ESI-MS/MS

The HILIC-enriched tryptic digest was separated with a nanoACQUITY UPLC system (Waters, Milford, MA) and analyzed using an LTQ Orbitrap Elite mass spectrometer (Thermo Scientific, Waltham, MA) equipped with a nano-electrospray source. Each 5 μl aliquot of the peptide solution was loaded into a nanoACQUITY UPLC Symmetry C18 column of i.d.180 μm, length 20 mm, and particle size 5 μm (Waters) using an autosampler. The homemade microcapillary separation column was packed with C18 material (Michrom Bioresources) in a fused-silica capillary [39]. The peptides trapped on the trap column after 10 min at a flow rate of 4 μl/min for desalting were back-flushed on a homemade microcapillary column (i.d. 100 μm and length 200 mm, C$_{18}$, 3 μm particle size, 100 Å pore size) for separation. Mobile phase A consisted of 100 % water containing 0.1 % FA. Mobile phase B was 100 % ACN containing 0.1 % FA. The LC gradient was 5 % B maintained from 0 to 15 min; then, the mobile phase B was increased to 15 % for 5 min, to 50 % B for 115 min, and to 95 % B for 21 min (95 % B was continued for 13 min). Phase B was then decreased to 5 % for 1 min. The column was re-equilibrated with 5 % B for 10 min before the next run. The electrospray voltage was set to 2.2 kV. The LTQ Orbitrap Elite mass spectrometer (Thermo Scientific) was operated in data-dependent mode during the chromatographic separation. The MS acquisition parameters for full-scan resolution was 60,000 in the Orbitrap for each sample; five data-dependent MS/MS scans were acquired by collision-induced dissociation (CID) and higher-energy collision dissociation (HCD) in each full scan. CID and HCD scans were acquired in linear trap quadrupole (LTQ) mode with a 30-ms activation time and in Orbitrap at resolution 15,000 with a 20-ms activation time, respectively. A 35 % normalized collision energy (NCE) was used for CID and HCD analyses. Previously fragmented ions were excluded for 300 s in all MS/MS scans.

N-Glycopeptide identification

We manually performed systematic identification using CID and HCD spectra, as shown in Fig. 1 [28]. Briefly, manual N-glycopeptide identification included the following steps. First, a target N-glycopeptide database was constructed from a combination of the tryptic peptides including 50 N-glycosylation sites without miscleavage referenced in the Uniprot database (http://www.uniprot.org) and the 331 N-linked glycans that are biologically possible [40]. Next, tandem MS spectra of the N-glycopeptides were selected from HCD spectra based on the presence of at least four unique oxonium ions from glycan fragmentation; these consisted of GlcNAc (m/z 138.1, 168.1, and 204.1), NeuAc (m/z 274.1, 292.1), and GlcNAc-Hex (m/z 366.1) [41, 42]. Tandem MS spectra of targeted N-glycopeptides were selected from HCD and CID spectra based on the presence of y- and b-ions from the fragmentation of the peptide backbone and the Y-series ions from N-glycopeptides. We defined the minimum requirement criteria using two or more fragments of y- and b-ions from the peptide backbone, as well as Y0, Y1, Y2, and

Y3-ions from the core N-glycopeptide glycan structure (Y0 = peptide_0_0_0_0 (Hex_HexNAc_Fuc_Sia), Y1 = peptide_0_1_0_0, Y2 = peptide_0_2_0_0 and _0_1_1_0, Y3 = peptide_0_2_1_0, _1_2_0_0 and _0_2_0_0). The y- and b-ions have been used with a relative intensity of more than 2 % (average S/N >3) and a mass accuracy with a tolerance less than 0.05 Da in HCD spectra. By comparing the theoretical monoisotopic ions in DB with the experimental monoisotopic ions in MS1, the target candidates were obtained from the HCD spectra of the selected N-glycopeptides. The N-glycopeptide candidates were then identified from the CID spectra by confirming the Y-series ions (Fig. 1b).

Results and discussion

Selection of target proteins and N-glycopeptides database construction

We previously examined the major proteins in HCC plasma, including AAT, HP, fetuin A (FETUA), alpha-1-antichymotrypsin (AACT), ceruloplasmin (CP), VTN, and alpha-1-acid glycoprotein 1/2 (AGP 1/2), and found indirect evidence of aberrant glycosylation using a specific lectin-coupled MRM assay [35–37]. Recent analyses of a single targeted protein showed that the N-glycopeptides of HP, kininogen-1 (KNG1), VTN, and immunoglobulin gamma isoforms (IgG1, 2, 3, and 4) were identified in HCC plasma [26–28, 43]. Additionally, large-scale analyses using tandem mass spectrometry have also been performed; however, few fucosylated N-glycopeptides were found in human sera [34, 44].

In this study, we selected 13 target proteins based on their abundance in human plasma [45] (Table 1). The protein concentration range of these 13 target proteins was 1–45 μmol/l [45].

In our recent study of vitronectin, a plasma protein, we provided a scheme for site-specific N-glycopeptide analysis of a single target protein [28]. To analyze various fucosylated glycoproteins in human plasma in this study, we modified the strategy for mapping the site-specific N-glycosylation of target proteins to include database construction, HILIC enrichment, LC-MS/MS analysis, and identification of N-glycopeptides (Fig. 1). For site-specific identification of various fucosylated N-glyco eptides from 13 highly abundant plasma proteins, we constructed, based on prior literature, a theoretical database of the mono-isotope ions of tryptic 16,550 N-glycopeptides from a combination of 50 tryptic peptides from 13 target proteins and 331 biologically possible N-linked glycans [40] (Fig. 1a).

Sample preparation and LC-MS/MS analysis

In this study, a pooled HCC plasma sample was prepared, tryptic-digested, and enriched using the HILIC method. The HILIC-enriched samples were analyzed in triplicate using a data-dependent acquisition mode in HCD/CID tandem mass spectrometry. The enriched samples obtained from depleted and non-depleted plasma were separated by reverse-phase nano-LC-MS/MS (Fig. 2a and ESM Fig. S1). The tryptic N-glycopeptides of target proteins were eluted in the range of 60–120 min. The glycopeptides identified from LC-MS/MS runs were further evaluated by their retention times. The relative standard deviation of the retention time was less than 1.2 %. The extracted ion chromatogram (XIC) showed different retention times for different glycopeptides from depleted plasma samples (Fig. 2b). The extracted ion chromatograms of six N-glycopeptides from $AALAAFNAQNN_{176}$ GSNFQLEEISR in FETUA (Fig. 2c) showed retention times that correlated with the type of glycan. Two sialylated N-glycopeptides, $AALAAFNAQNN_{176}GSNFQLEEISR\_5\_4\_0\_1$ (5Hex_4HexNAc_0Fuc_1Sia) and $AALAAFNAQNN_{176}$ GSNFQLEEISR_5_4_0_2 (5Hex_4HexNAc_0Fuc_2Sia), had different retention times, at 81.29 and 83.87 min, respectively, which were dependent on the number of sialic acids. The more sialylated the N-glycopeptide, the longer it was retained in RP-LC [46]. However, the fucosylated N-glycopeptides, including $AALAAFNAQNN_{176}GSNF$ QLEEISR_5_4_1_2 (5Hex_4HexNAc_1Fuc_2Sia) and $AALAAFNAQNN_{176}GSNFQLEEISR\_6\_5\_1\_3$ (6Hex_5HexNAc_1Fuc_3Sia), showed the same retention times (83.69 and 85.36 min, respectively) as their corresponding non-fucosylated N-glycopeptides, $AALAAFNAQ$ $NN_{176}GSNFQLEEISR\_5\_4\_0\_2$ (5Hex_4HexNAc_ 0Fuc_2Sia) and $AALAAFNAQNN_{176}GSNFQ$ LEEISR_6_5_0_3 (6Hex_5HexNAc_0Fuc_3Sia). This is because these isoforms have an equal number of sialic acids. When the peptide backbones in N-glycopeptides were identical, the N-glycopeptides, with one exception, were eluted at similar retention times in reverse-phase liquid chromatography. When the glycopeptides had sialic acids, we considered the retention time to be a direct reflection of the number of sialic acids.

Identification of target N-glycopeptides in plasma

Using the systematic workflow to interpret HCD and CID spectra [28] (Fig. 1b), 189 unique N-glycopeptides were identified from human plasma samples (ESM Table S2). We manually assigned all the y-, b-, Y-, B-, and oxonium ions in the HCD and CID spectra of the target N-glycopeptides for positive identification. The Y-ion series are fragments from glycopeptides containing a glycan structure on a peptide backbone. The total MW of the Y-ion series from N-glycopeptides
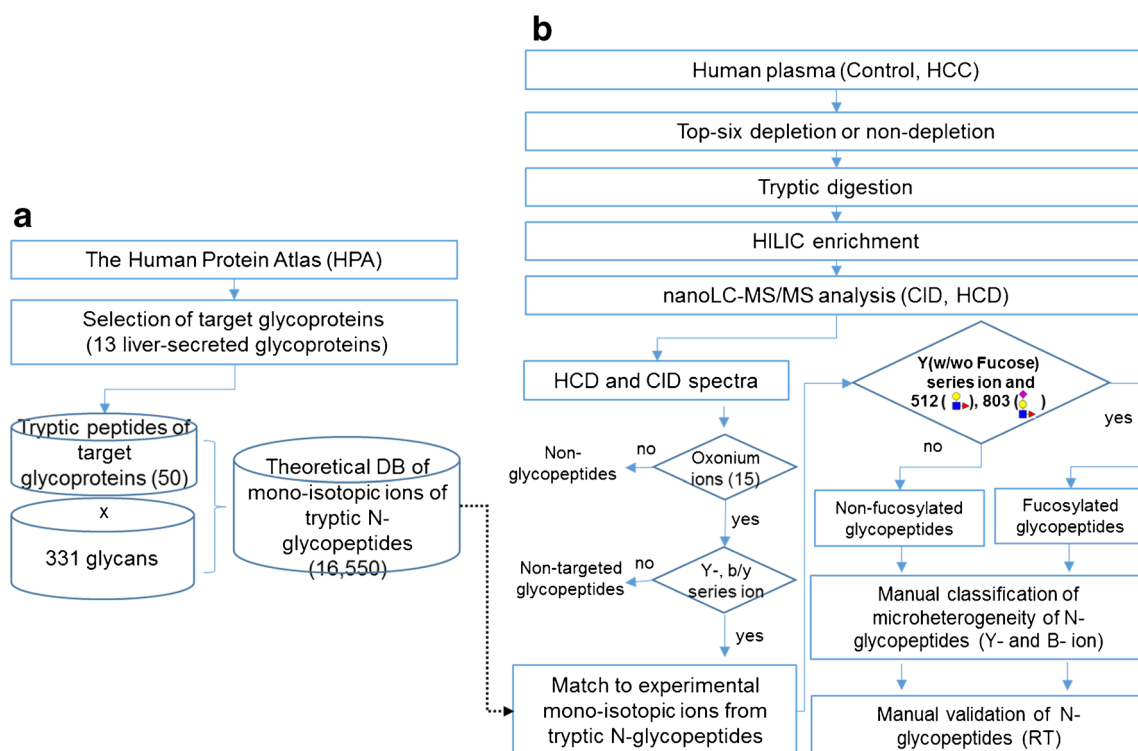
Fig. 1 Strategy for the mapping of site-specific N-glycosylation of target proteins from human plasma. (**a**) Selection of target proteins and construction of theoretical tryptic N-glycopeptides DB. (**b**) Identification of target N-glycopeptides by LC/MS/MS

consists of glycans and peptides. Because we know the theoretical MWs of the 331 N-linked glycans that are biologically possible, we can match the theoretical MWs of peptides using the Uniprot database, which can then be compared with the experimental MWs of the peptides (= (Total MW of Y-ion series) − (MW of glycans)) using a fingerprinting method. Therefore, we can use the Y-ion series for the identification of N-glycopeptides in the HCD and CID spectra using the limited database. The following example illustrates the step-by-step assignments of tandem MS spectra from fucosylated

Table 1 Selection of 13 liver-secreted proteins from human plasma

No.	Glycoproteins	Acronym	Uniprot accession number	Concentration range in plasma (μmol/l)[a]	Transcript abundance in liver tissue[b] (organ highly expressed)	Detected in non-depleted plasma	Detected in depleted plasma
2	Alpha-1-antitrypsin	AAT	P01009	18–40	High (liver)	√	n.d.
3	Alpha-2-HS-glycoprotein	FETUA	P02765	9–30	High (liver)	√	√
4	Ceruloplasmin	CP	P00450	2–5	High (liver)	√	√
5	Haptoglobin	HP	P00738	6–40	High (liver)	√	n.d.
6	Kininogen-1	KNG1	P01042	3	High (liver)	√	√
7	Vitronectin	VTN	P04004	1–3	High (liver)	√	√
8	Alpha-1-acid glycoprotein 1	AGP1	P02763	9–20	High (liver)	√	√
9	Alpha-1-acid glycoprotein 2	AGP2	P19652	4–10	High (liver)	√	√
10	Alpha-2-macroglobulin	A2M	P01023	7–17	Medium (lung)	√	√
11	Hemopexin	HPX	P02790	9–20	High (liver)	√	√
12	Serotransferrin	TF	P02787	25–45	High (liver)	√	n.d.
13	Beta-2-glycoprotein 1	APOH	P02749	3–6	High (liver)	√	√

[a] Protein concentration in human plasma [45]

[b] Calculated as (transcript abundance in liver /transcript abundance in organ highly expressed) × 100 [11]

n.d.: not detected

N-glycopeptides. FETUA has two N-glycosylation sites, at N176 and N156, with tryptic glycopeptide sequences of AALAAFNAQNN$_{176}$GSNFQLEEISR and VCQDCP LLAPLN$_{156}$DTR, respectively. A recent study reported two N-glycopeptides after a site-specific analysis using acetone enrichment and LC/MS [44]. They identified only one FETUA N-glycopeptide, which consisted of only a bi-antennary type, in sera [44]. However, we found nine bi- and tri-antennary-type N-glycopeptides (ESM Table S2). Figure 3 shows the typical tandem MS spectra of FETUA fucosylated N-glycopeptides containing AALAA FNAQNN$_{176}$GSNFQLEEISR_5_4_0_2 (5Hex_4HexNAc_0Fuc_2Sia) and AALA AFNAQNN$_{176}$GSNFQLEEISR_5_4_1_2 (5Hex_ 4HexNAc_1Fuc_2Sia) in plasma. The candidate N-glycopeptides were first selected using oxonium ions from the glycan fragmentation in the HCD spectra. The peptide backbone of the N-glycopeptides was confirmed by the existence of y- and b-series ions from the peptide fragmentation in the HCD spectra. The N-glycopeptides with the same peptide backbone usually showed similar HCD spectra because they share the b- and y-series ions in HCD mode (Fig. 3a).

To find fucosylated N-glycopeptides, we used B-series ions at m/z 512.36 (1Hex_1HexNAc_1Fuc_0Sia) and m/z 803.53 (1Hex_1HexNAc_1Fuc_1Sia) and/or Y-series ion pairs with/without fucose in CID mode (Fig. 1b). The CID spectrum of fucosylated N-glycopeptides, such as AALA AFNAQNN$_{176}$GSNFQLEEISR_5_4_1_2 (5Hex_ 4HexNAc_1Fuc_2Sia), showed B-series ions at m/z 512.36 and 803.53 and nine different pairs of Y-series ions with/without fucose (Fig. 3b).

By systematically interpreting the CID and HCD tandem mass spectra, we profiled target proteins of N-glycopeptides in human plasma. In total, 189 N-glycopeptides from 32 glycosylated sites on 13 major proteins were identified in plasma samples (ESM Table S2). The molecular ions of identified N-glycopeptides were confirmed with less than 10 ppm mass error.

The identified N-glycopeptides were classified as bi-antennary- (42.8 %), tri-antennary- (39.7 %), tetra-antennary- (9.5 %), mono-antennary- (6.3 %), hybrid- (2.1 %), or high-mannose- (0.5 %) type glycoforms in HCC plasma (Fig. 4a). Non-fucosylated and fucosylated N-glycopeptides were then split into two groups (Fig. 4b and c, respectively). The glycoform pattern of the non-fucosylated N-glycopeptides was similar to those of total N-glycopeptides (Fig. 4b). However, the fucosylated N-glycopeptides showed different tri-, bi-, and tetra-antennary glycoform percentages (48, 42, and 10 %, respectively) (Fig. 4c). Recently, Wuhrer et al. reviewed glycomic studies of major human plasma glycoproteins, including alpha-1-acid glycoprotein, alpha-1-antitrypsin, fetuin A, alpha-2-macroglobulin, ceruloplasmin, haptoglobin, kininogen-1, vitronectin, hemopexin, serotrans

ferrin, and beta-2-glycoprotein 1 [47]. In their report, bi-antennary and tri-antennary complex-type glycoforms with/without fucose were the dominant glycoforms of the target plasma proteins, which is similar to the results of this study.

In contrast, mono-antennary glycoforms with only three N-acetylhexoseamine residues were more common in our study than in that performed by Clerc et al. (ESM Table S3). More recently, Reusch et al. reported that in-source decay may occur in all MS-based methods [48]. In their report, the mono-antennary glycoforms were relatively quantified at less than 10 %, based on various MS-based methods, and the loss of an antenna from bi-antennary glycoforms generally occurred with a charge reduction in ESI-source-based MS analysis [48]. Therefore, it is possible that the mono-antennary glycoforms found in the present study were partly formed by in-source decay.

The glycoprotein fucosylation level increases with the progression of liver cancer [49], and this idea has received significant attention in biomarker studies. In this study, we identified 71 fucosylated N-glycopeptides from 13 major human plasma proteins (Table 2, ESM Fig. S2). Additionally, we identified 37 new fucosylated N-glycopeptides from AACT, AAT, FETUA, CP, AGP 1/2, alpha-2-macroglobulin (A2M), serotransferrin (TF), and beta-2-glycoprotein 1 (APOH) in plasma. We focused primarily on the major abundant proteins in human plasma using our systematic workflow, which rigorously searches fucose-related B-series ions (m/z 512.36 and m/z 803.53) as well as Y-series ion pairs with/without fucose from among possible candidate glycopeptide spectra; this approach detected more fucosylated N-glycopeptides from target proteins than any other method to date [26, 33, 34, 43, 44].

Of the 13 liver-secreted glycoproteins in HCC plasma, all N-glycopeptides from 32 N-glycosylation sites were classified as site-specific glycoforms of fucosylated and non-fucosylated glycopeptides (Fig. 5). All the N-glycosylation sites were fully determined from the N-glycopeptides of FETUA, KNG, and VTN, whereas those of AACT, AAT, HP, CP, AGP 1/2, A2M, hemopexin (HPX), TF, and APOH were partially determined.

Most HCC plasma N-glycopeptides were identified as bi- and tri-antennary types, whereas tri- and tetra-antennary types

Fig. 2 LC/MS chromatograms of tryptic peptides from a depleted ▶ plasma sample. (**a**) Base peak chromatogram (BPC) of total peptides from plasma in triplicate runs. (**b**) Extracted ion chromatogram (XIC) of identified N-glycopeptides from target proteins. (**c**) XIC of two fucosylated and four non-fucosylated N-glycopeptides with N176 glycosylation site from fetuin **a**. As an example, pep_5_4_0_2 represents peptide_5Hex_4HexNAc_0Fuc_2Sia. pep = AALA…R (AALAAFNAQNN$_{176}$GSNFQLEEISR); *green circle*, mannose; *yellow circle*, galactose; *blue square*, N-acetylglucosamine; *red triangle*, fucose; *purple diamond*, sialic acid
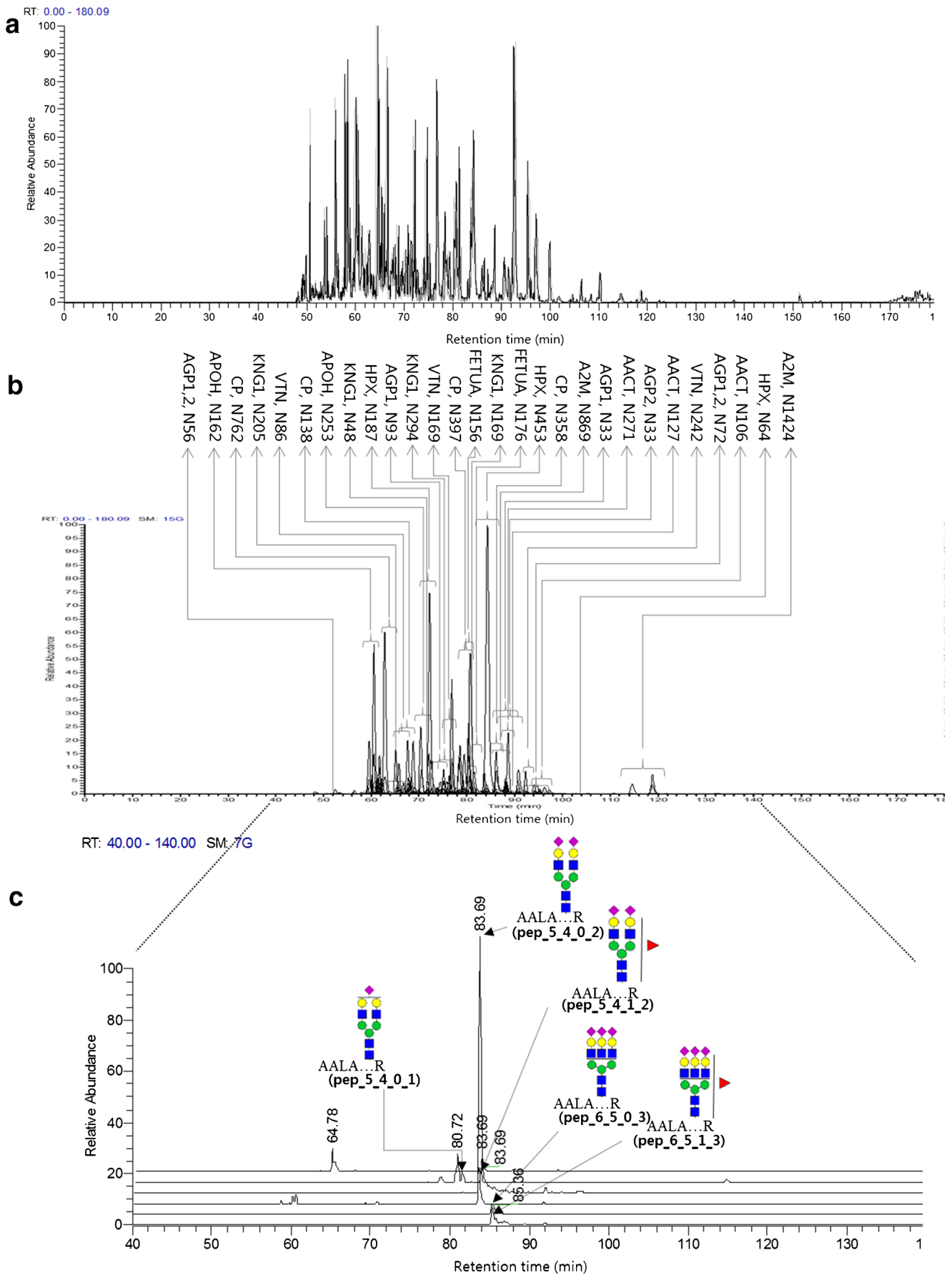
Fig. 3 LC/MS/MS spectra of non-fucosylated and fucosylated N-glycopeptides, AALAAFN AQNNGSN$_{176}$FQLEEISR_5_4_ 0_2 (5Hex_4HexNAc_0Fuc_ 2Sia) and AALAAFNAQ NNGSN$_{176}$FQLEEISR_5_4_1_ 2, containing N176 site of fetuin A from Fig. 2C. **a** HCD spectra of non-fucosylated (*top*) and fucosylated (*bottom*) N-glycopeptides. **b** CID spectra of non-fucosylated (*top*) and fucosylated (*bottom*) N-glycopeptides. The *black arrow* indicates oxonium ions, and the *purple arrow* indicates y- and b-ions fragmented from the peptide. The *blue arrow* indicates Y-series fragment ions from N-glycopeptides, the *red arrow* indicates Y-series fragment ions containing fucose, and the *black square box* indicates a pair of fragment ions containing fucose and non-fucose. As an example, pep_5_4_0_2 represents peptide_ 5Hex_4HexNAc_0Fuc_2Sia. pep = AALA…R (AALAAF NAQNN$_{176}$GSNFQLEEISR); *green circle*, mannose; *yellow circle*, galactose; *blue square*, N-acetylglucosamine; *red triangle*, fucose; *purple diamond*, sialic acid
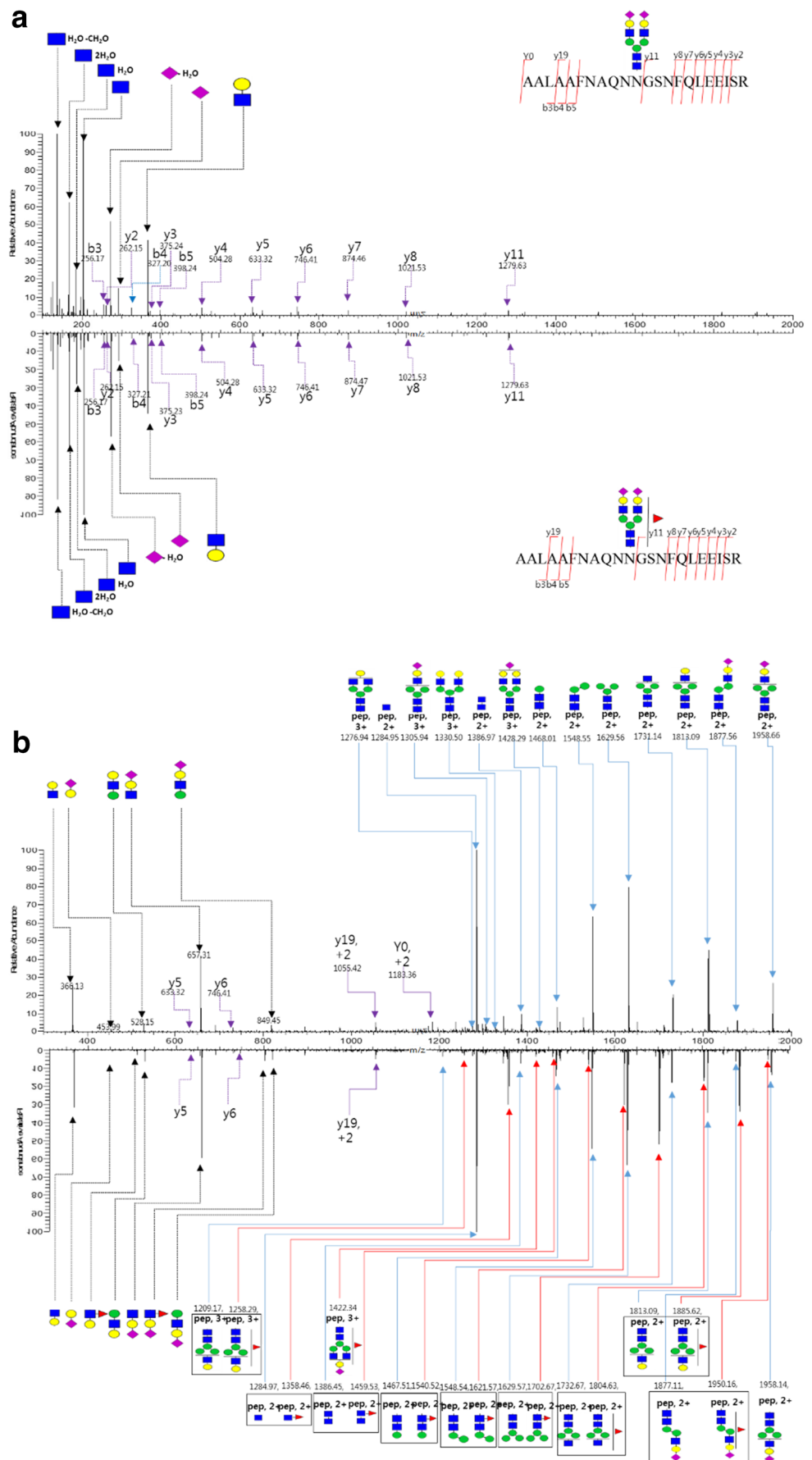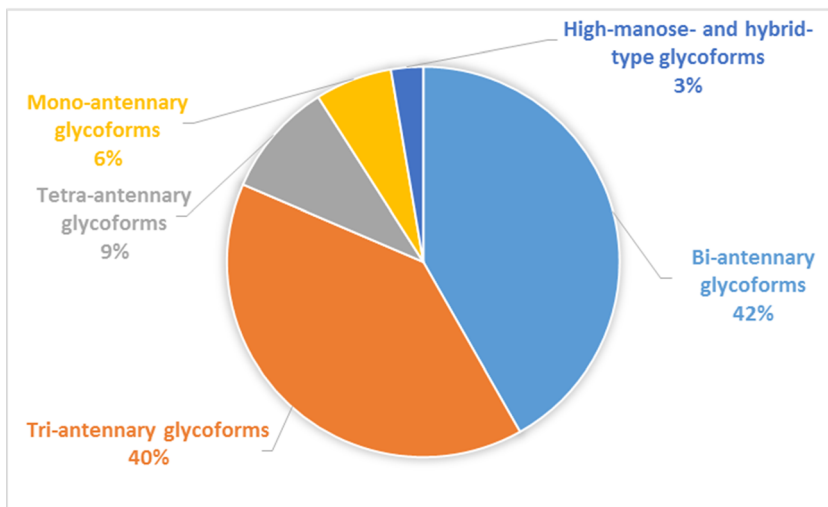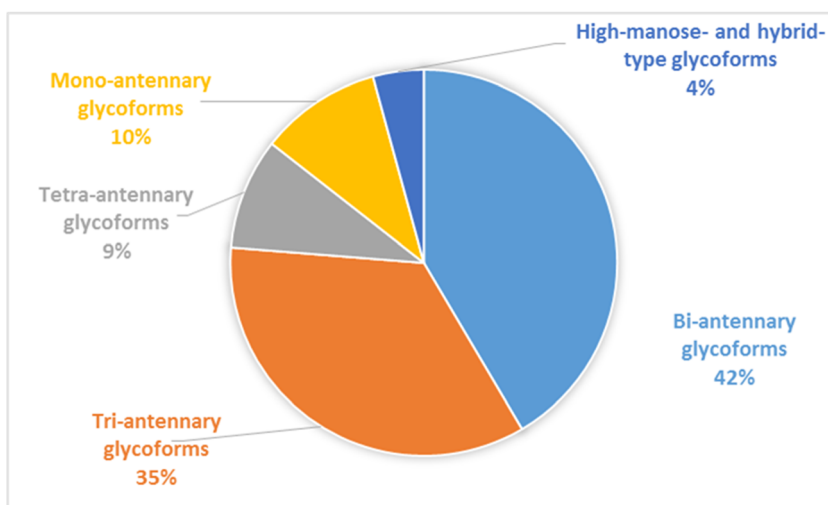
Fig. 4 Pie charts of glycoform classification, including bi-antennary, tri-antennary, tetra-antennary, mono-antennary, hybrid-, and high-mannose-type glycoforms. **a** Total identified N-glycopeptides; **b** non-fucosylated N-glycopeptides; and **c** fucosylated glycopeptides in hepatocellular carcinoma plasma

a Total N-glycopeptides

High-manose- and hybrid-type glycoforms 3%

Mono-antennary glycoforms 6%

Tetra-antennary glycoforms 9%

Bi-antennary glycoforms 42%

Tri-antennary glycoforms 40%

b Non-fucosylated N-glycopeptides

High-manose- and hybrid-type glycoforms 4%

Mono-antennary glycoforms 10%

Tetra-antennary glycoforms 9%

Bi-antennary glycoforms 42%

Tri-antennary glycoforms 35%

c Fucosylated N-glycopeptides

Tetra-antennary glycoforms 10%

Bi-antennary glycoforms 42%
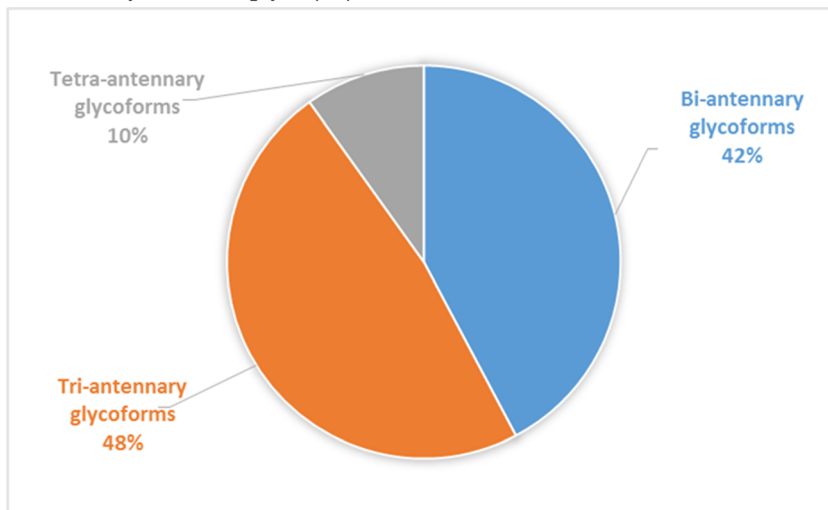
Tri-antennary glycoforms 48%

Table 2 List of tryptic N-glycopeptides with fucose from 13 human plasma proteins

No.	Acronym	Glyco-site	Glycopeptides (pep_Hex_HexNAc_Fuc_Sia)	Charge state	Theo. *m/z*	Exp. *m/z*	Mass error (ppm)	Average RT	Reference
1	AACT	N106	FNLT…R_6_5_1_3	4+	1352.567	1352.573	4.31	95.14	New
				5+	1082.255	1082.258	2.66	95.19	
			FNLT…R_7_6_1_3	4+	1443.850	1443.856	4.24	94.66	[1]
		N271	YTGN…K_6_5_1_2	3+	1490.284	1490.290	4.29	84.93	New
			YTGN…K_6_5_1_3	3+	1587.315	1587.323	4.75	87.88	New
				4+	1190.738	1190.744	4.60	88.01	
			YTGN…K_7_6_1_4	4+	1354.795	1354.801	3.93	90.21	New
			YTGN…K_7_6_2_3	4+	1318.536	1318.542	4.57	87.35	New
2	AAT	N271	YLGN…K_5_4_1_1	3+	1272.547	1272.558	8.64	93.26	New
			YLGN…K_5_4_1_2	3+	1369.578	1369.586	5.57	96.75	New
3	FETUA	N176	AALA…R_5_4_1_2	3+	1572.664	1572.670	4.11	83.23	New
			AALA…R_6_5_1_3	4+	1343.806	1343.813	4.52	85.29	New
		N156	VCQD…R_5_4_1_2	3+	1374.895	1374.901	4.27	80.33	New
			VCQD…R_6_5_1_3	4+	1195.480	1195.484	2.89	82.75	New
4	CP	N358	AGLQ…K_5_4_1_2	3+	1330.876	1330.881	3.21	86.02	New
		N138	EHEG…R_5_4_1_1	3+	1318.195	1318.200	3.74	63.46	[2]
			EHEG…R_5_4_1_2	3+	1415.227	1415.232	3.79	65.17	[1, 2, 5]
				4+	1061.672	1061.676	3.60	65.02	
			EHEG…R_6_5_1_3	4+	1225.729	1225.735	4.75	66.79	[1, 5]
		N762	ELHH…K_5_4_1_1	3+	1361.249	1361.255	4.36	68.48	New
			ELHH…K_5_4_1_2	3+	1458.281	1458.287	4.23	68.75	[1, 2]
				4+	1093.963	1093.967	3.77	68.62	
			ELHH…K_6_5_1_2	4+	1185.246	1185.251	4.24	68.51	[2]
			ELHH…K_6_5_1_3	4+	1258.019	1258.025	4.43	70.29	[1]
		N397	ENLT…R_5_4_1_2	3+	1493.279	1493.285	3.84	80.26	[2]
				4+	1120.211	1120.217	4.62	80.16	
			ENLT…R_6_5_1_3	4+	1284.268	1284.272	3.17	81.98	[2]
5	HP	N241	VVLH…K_5_4_1_2	3+	1382.617	1382.625	5.93	81.64	[4]
			VVLH…K_6_5_1_3	4+	1201.271	1201.278	5.27	83.60	[1, 2, 4]
6	KNG1	N169	HGIQ…K_6_5_1_3	4+	1407.832	1407.838	4.07	83.68	[4]
		N205	ITYS…K_6_5_1_2	3+	1377.225	1377.231	4.14	65.85	[4]
			ITYS…K_6_5_1_3	3+	1474.257	1474.264	4.70	67.78	[4]
		N294	LNAE…K_5_4_1_2	3+	1261.510	1261.516	4.97	74.71	[4]
			LNAE…K_6_5_1_2	3+	1383.221	1383.226	4.19	74.28	[4]
			LNAE…K_6_5_1_3	3+	1480.252	1480.257	3.47	76.50	[4]
7	VTN	N242	NISD…R_5_4_1_2	4+	1281.542	1281.548	4.31	92.09	[2, 3]
			NISD…R_6_5_1_3	4+	1445.599	1445.604	3.82	94.19	[2, 3, 5]
		N86	NNAT…K_6_5_1_3	4+	1347.810	1347.818	5.69	68.55	[2, 3]
8,9	AGP1	N33	LVPV…K_5_4_1_2	3+	1377.621	1377.620	2.66	88.65	New
			LVPV…K_6_5_1_2	3+	1499.332	1499.330	4.29	87.99	New
				4+	1124.751	1124.749	4.04	87.98	New
			LVPV…K_6_5_1_3	3+	1596.364	1596.362	4.90	90.65	New
				4+	1197.525	1197.523	3.34	90.64	New
			LVPV…K_6_5_2_2	3+	1548.018	1548.016	0.88	87.73	New
			LVPV…K_6_5_2_3	4+	1234.039	1234.038	2.12	90.68	New
		N93	QDQC…R_6_5_1_3	3+	1641.655	1641.654	3.77	98.84	[1]
			QDQC…R_7_6_1_2	4+	1250.003	1250.001	3.25	95.17	[1]
			QDQC…R_7_6_1_3	4+	1322.777	1322.775	3.18	98.38	[1]

Table 2 (continued)

| No.	Acronym	Glyco-site	Glycopeptides (pep_Hex_HexNAc_Fuc_Sia)	Charge state	Theo. *m/z*	Exp. *m/z*	Mass error (ppm)	Average RT	Reference
			QDQC…R_7_6_2_3	4+	1359.291	1359.289	2.09	94.94	New
	AGP1,2	N72	SVQE…K_7_6_1_2	4+	1251.017	1251.015	5.58	93.14	New
	AGP2	N33	LVPV…R_6_5_1_1	3+	1278.565	1278.569	3.08	73.76	New
			LVPV…R_6_5_1_2	3+	1375.597	1375.601	3.37	76.15	New
				4+	1031.949	1031.953	3.61	76.17	New
			LVPV…R_6_5_1_3	3+	1472.628	1472.635	4.64	78.40	New
				4+	1104.723	1104.728	3.78	78.39	New
10	A2M	N1424	VSNQ…R_5_4_1_0	3+	1311.277	1311.280	4.58	110.79	[2]
			VSNQ…R_5_4_1_1	3+	1408.308	1408.315	4.64	114.58	[5]
				4+	1056.483	1056.487	4.29	114.58	
			VSNQ…R_5_4_1_2	3+	1505.340	1505.346	4.23	118.86	[1]
				4+	1129.257	1129.260	3.70	118.48	
			VSNQ…R_5_4_2_1	3+	1456.994	1457.002	5.75	114.36	New
				4+	1092.997	1093.001	3.36	114.39	
			VSNQ…R_5_5_1_0	3+	1378.970	1378.975	4.35	110.80	New
			VSNQ…R_5_5_1_1	4+	1107.253	1107.256	2.78	114.44	New
			VSNQ…R_6_5_1_1	3+	1530.019	1530.026	4.51	114.03	New
				4+	1147.766	1147.772	4.60	114.03	
			VSNQ…R_6_5_1_2	4+	1220.540	1220.545	4.69	117.93	[2, 5]
11	HPX	N453	ALPQ…H_5_4_1_1	3+	1265.875	1265.881	4.20	81.25	[4]
			ALPQ…H_5_4_1_2	3+	1362.907	1362.914	4.93	84.35	[4]
		N187	SWPA…R_5_4_1_1	3+	1155.472	1155.477	4.31	69.71	[2, 4]
			SWPA…R_5_4_1_2	3+	1252.504	1252.509	4.06	72.06	[1, 2, 4, 5]
			SWPA…R_6_5_1_2	3+	1374.214	1374.219	3.24	71.63	[4]
			SWPA…R_6_5_1_3	3+	1471.246	1471.252	4.25	73.76	[4]
12	TF	N432	CGLV…K_5_4_1_1	3+	1179.499	1179.505	4.87	77.31	New
			CGLV…K_5_4_1_2	3+	1276.531	1276.538	5.13	80.37	[6]
			CGLV…K_6_5_1_2	3+	1398.242	1398.251	6.23	80.15	New
		N630	QQQH…R_5_4_1_2	4+	1217.244	1217.250	5.17	86.23	[1, 6]
			QQQH…R_6_5_1_3	4+	1381.300	1381.310	6.81	88.67	New
13	APOH	N253	LGNW…K_5_4_1_2	3+	1201.136	1201.141	4.29	70.03	New
			LGNW…K_6_5_1_3	3+	1419.878	1419.883	3.04	71.88	New
		N162	VYKP…R_5_4_1_1	3+	1176.834	1176.837	2.35	59.18	New
			VYKP…R_5_4_1_2	3+	1273.866	1273.869	2.64	60.56	[1, 7]
			VYKP…R_6_5_1_3	3+	1492.608	1492.613	3.24	61.71	[7]
				4+	1119.708	1119.712	3.28	61.71	
			VYKP…R_6_5_2_3	3+	1541.294	1541.300	3.67	61.67	New

Reference: (1) Takakura D et al. [43], (2) Mayampurath A et al. [34], (3) Hwang H et al. [28], (4) Pompach P et al. [26], (5) Mayampurath A et al. [33], (6) Satomi Y et al. [52], and (7) Kondo A et al. [51]

New fucose-containing glycopeptides newly identified in this report, *n.d.* not detected

were mainly identified for AACT and AGP. Previous studies have shown that tetra-antennary glycoforms are common for AGP [47, 50]. All the N-glycopeptides identified from HPX, TF, and APOH were bi- and tri-antennary glycoforms. A previous study showed that bi- and tri-antennary glycoforms of the N162 site in APOH were mainly identified in the serum from patients with antiphospholipid syndrome [51]. The fucosylated N-glycopeptides from KNG, FETUA, CP, TF, and APOH were classified as bi- and tri-antennary types. The N241 site of HP was determined to form bi- and tri-antennary-type glycoforms. In a previous study, Goldman et al. identified similar bi- and tri-antennary-type glycoform

Fig. 5 A global map of fucosylated and non-fucosylated glycopeptides from 13 liver-secreted glycoproteins in hepatocellular carcinoma plasma. a Total identified N-glycopeptides; b non-fucosylated N-glycopeptides; and c fucosylated glycopeptides
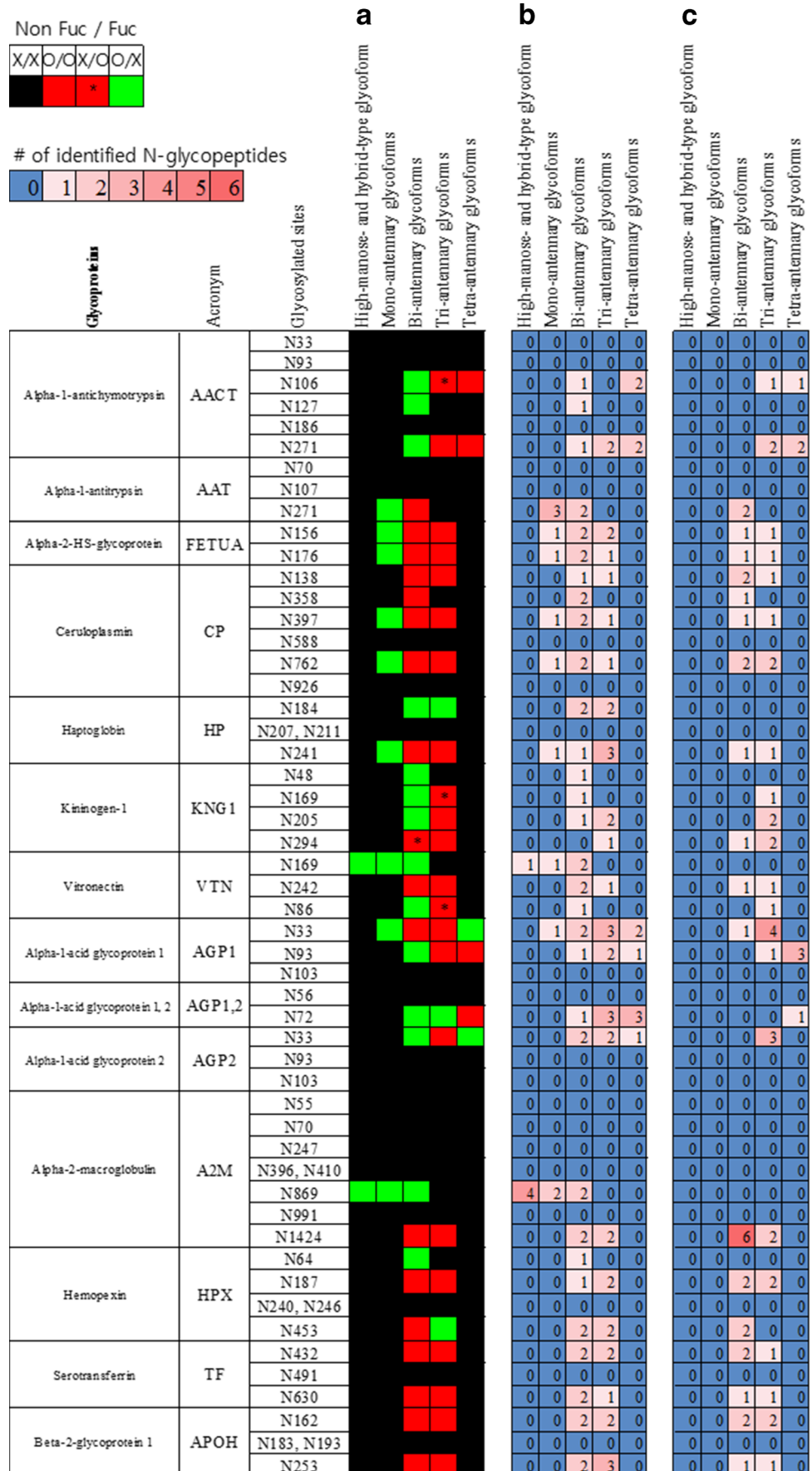
patterns for HP, KNG, and HPX after neuraminidase treatment [26]. The N432 and N630 sites of TF formed bi- and tri-antennary-type glycoforms; however, no alteration of the N491 site was detected, and this site had been previously shown to have low levels of glycosylation [47, 52]. Hybrid-type glycoforms were identified at N169 of VTN and N869 of A3M. High-mannose-type glycoforms were detected at N869 of A2M [53], and hybrid-type glycoforms were detected at N169 of VTN [28, 47]. These results demonstrated that site-specific N-glycopeptide analysis is important in the study of glycoproteins.

Goldman et al. concluded that the relative distribution of fucosylated N-glycopeptides is protein- and site-specific [26]. The site-specific micro-heterogeneity of fucosylation depends on the activity and stability of fucosyltransferases, such as Fut 8 and/or Fut 6 [5–7], the sequence of glycosyltransferase action, and the protein structure [26]. The limitations of a glycomics approach are apparent in the research with complex samples. Therefore, site-specific N-glycopeptide analysis is necessary for the study of fucosylated glycoproteins in complex samples, such as human HCC plasma.

Conclusions

In this study, we identified site-specific fucosylation of N-glycopeptides from HCC plasma samples. In total, 189 N-glycopeptides from 13 liver-secreted proteins, including 71 fucosylated N-glycopeptides, were identified. The fucosylated N-glycopeptides consisted of tri- (48 %), bi- (42 %), and tetra- (10 %) antennary glycoforms. In this study, 37 fucosylated N-glycopeptides, mostly consisting of bi- and tri-antennary glycoforms, were newly identified in HCC plasma samples. Of particular interest were the tetra- and tri-antennary glycoforms from AACT and AGP. We obtained a list of various fucosylated N-glycopeptides from liver-secreted proteins in human HCC plasma. These fucosylated N-glycopeptides could be used for the quantitation of site-specific fucosylation in HCC plasma proteins. As a next step, using multiple reaction monitoring, we will attempt to analyze differential fucosylation in liver-secreted proteins in various plasma samples from patients with various types of cancer.

Compliance with ethical standards

Conflict of interest The authors have no conflicts of interest to declare.

Ethics approval and consent to participate This study was performed in accordance with ethical standards. Plasma samples were obtained from voluntary blood donors with informed consent and approval in accordance with IRB guidelines from Yonsei University College of Medicine (Seoul, Korea).

References

1. Walsh G, Jefferis R. Post-translational modifications in the context of therapeutic proteins. Nat Biotechnol. 2006;24(10):1241–52.
2. Kornfeld R, Kornfeld S. Assembly of asparagine-linked oligosaccharides. Annu Rev Biochem. 1985;54(1):631–64.
3. An HJ, Peavy TR, Hedrick JL, Lebrilla CB. Determination of N-glycosylation sites and site heterogeneity in glycoproteins. Anal Chem. 2003;75(20):5628–37.
4. Fuster MM, Esko JD. The sweet and sour of cancer: glycans as novel therapeutic targets. Nat Rev Cancer. 2005;5(7):526–42.
5. Cheng L, Luo S, Jin C, Ma H, Zhou H, Jia L. FUT family mediates the multidrug resistance of human hepatocellular carcinoma via the PI3K/Akt signaling pathway. Cell Death Dis. 2013;4(11):e923. doi:10.1038/cddis.2013.450.
6. Kang X, Wang N, Pei C, Sun LU, Sun R, Chen JIE, et al. Glycan-related gene expression signatures in human metastatic hepatocellular carcinoma cells. Exp Ther Med. 2012;3(3):415–22.
7. Nakagawa T, Uozumi N, Nakano M, Mizuno-Horikawa Y, Okuyama N, Taguchi T, et al. Fucosylation of N-glycans regulates the secretion of hepatic glycoproteins into bile ducts. J Biol Chem. 2006;281(40):29797–806.
8. Anderson NL, Anderson NG. The human plasma proteome: history, character, and diagnostic prospects. Mol Cell Proteomics. 2002;2(1):847–67.
9. Farrah T, Deutsch EW, Omenn GS, Campbell DS, Sun Z, Bletz JA, et al. High-confidence human plasma proteome reference set with estimated concentrations in PeptideAtlas. Mol Cell Proteomics. 2011;10(9), M110.006353.
10. Boron WF, Boulpaep EL. Medical physiology: a cellular and molecular approach. Philadelphia: Elsevier/Saunders; 2003. p. 1300.
11. Uhlén M, Fagerberg L, Hallström BM, Lindskog C, Oksvold P, Mardinoglu A, et al. Proteomics. Tissue-based map of the human proteome. Science. 2015;6220(6220):1260419.
12. Ludwig JA, Weinstein JN. Biomarkers in cancer staging, prognosis and treatment selection. Nat Rev Cancer. 2005;5(11):845–56.
13. Miyaaki H, Nakashima O, Kurogi M, Eguchi K, Kojiro M. Lens culinaris agglutinin-reactive alpha-fetoprotein and protein induced by vitamin K absence II are potential indicators of a poor prognosis: a histopathological study of surgically resected hepatocellular carcinoma. J Gastroenterol. 2007;42(12):962–8.
14. Khien VV, Mao HV, Chinh TT, Ha PT, Bang MH, Lac BV, et al. Clinical evaluation of lentil lectin-reactive alpha-fetoprotein-L3 in histology-proven hepatocellular carcinoma. Int J Biol Markers. 2001;16(2):105–11.
15. Breborowicz J, Mackiewicz A, Breborowicz D. Microheterogeneity of alpha-fetoprotein in patient serum as demonstrated by lectin affino-electrophoresis. Scand J Immunol. 1981;14(1):15–20.
16. Okuda H, Saito A, Shiratori K, Yamamoto M, Takasaki K, Nakano M. Clinicopathologic features of patients with primary malignant hepatic tumors seropositive for alpha-fetoprotein-L3 alone in comparison with other patients seropositive for alpha-fetoprotein-L3. J Gastroenterol Hepatol. 2005;20(5):759–64.
17. Naitoh A, Aoyagi Y, Asakura H. Highly enhanced fucosylation of serum glycoproteins in patients with hepatocellular carcinoma. J Gastroenterol Hepatol. 1999;14(5):436–45.

18. Li D, Mallory T, Satomura S. AFP-L3: a new generation of tumor marker for hepatocellular carcinoma. Clin Chim Acta. 2001;313(1-2):15–9.

19. Taylor AD, Hancock WS, Hincapie M, Taniguchi N, Hanash SM. Towards an integrated proteomic and glycomic approach to finding cancer biomarkers. Genome Med. 2009;1(6):57.

20. Zhao J, Qiu W, Simeone DM, Lubman DM. N-linked glycosylation profiling of pancreatic cancer serum using capillary liquid phase separation coupled with mass spectrometric analysis. J Proteome Res. 2007;6(3):1126–38.

21. Pedersen JW, Blixt O, Bennett EP, Tarp MA, Dar I, Mandel U, et al. Seromic profiling of colorectal cancer patients with novel glyco-peptide microarray. Int J Cancer. 2011;128(8):1860–71.

22. Barrabés S, Pagès-Pons L, Radcliffe CM, Tabarés G, Fort E, Royle L, et al. Glycosylation of serum ribonuclease 1 indicates a major endothelial origin and reveals an increase in core fucosylation in pancreatic cancer. Glycobiology. 2007;17(4):388–400.

23. Comunale MA, Lowman M, Long RE, Krakover J, Philip R, Seeholzer S, et al. Proteomic analysis of serum associated fucosylated glycoproteins in the development of primary hepato-cellular carcinoma. J Proteome Res. 2006;5(2):308–15.

24. Schiel JE, Au J, He H-J, Phinney KW. LC-MS/MS biopharmaceu-tical glycoanalysis: identification of desirable reference material characteristics. Anal Bioanal Chem. 2012;403(8):2279–89.

25. Pompach P, Brnakova Z, Sanda M, Wu J, Edwards N, Goldman R. Site-specific glycoforms of haptoglobin in liver cirrhosis and hepa-tocellular carcinoma. Mol Cell Proteomics. 2013;12(5):1281–93.

26. Pompach P, Ashline DJ, Brnakova Z, Benicky J, Sanda M, Goldman R. Protein and site specificity of fucosylation in liver-secreted glycoproteins. J Proteome Res. 2014;13(12):5561–9.

27. Lee H-J, Cha H-J, Lim J-S, Lee SH, Song SY, Kim H, et al. Abundance-ratio-based semiquantitative analysis of site-specific N-linked glycopeptides present in the plasma of hepatocellular car-cinoma patients. J Proteome Res. 2014;13(5):2328–38.

28. Hwang H, Lee JY, Lee HK, Park GW, Jeong HK, Moon MH, et al. In-depth analysis of site-specific N-glycosylation in vitronectin from human plasma by tandem mass spectrometry with immuno-precipitation. Anal Bioanal Chem. 2014;406(30):7999–8011.

29. Kuo C-W, Wu I-L, Hsiao H-H, Khoo K-H. Rapid glycopeptide enrichment and N-glycosylation site mapping strategies based on amine-functionalized magnetic nanoparticles. Anal Bioanal Chem. 2012;402(9):2765–76.

30. Zhao Y, Yu L, Guo Z, Li X, Liang X. Reversed-phase depletion coupled with hydrophilic affinity enrichment for the selective iso-lation of N-linked glycopeptides by using Click OEG-CD matrix. Anal Bioanal Chem. 2011;399(10):3359–65.

31. Zhu J, Lin Z, Wu J, Yin H, Dai J, Feng Z, et al. Analysis of serum haptoglobin fucosylation in hepatocellular carcinoma and liver cir-rhosis of different etiologies. J Proteome Res. 2014;13(6):2986–97.

32. Asazawa H, Kamada Y, Takeda Y, Takamatsu S, Shinzaki S, Kim Y, et al. Serum fucosylated haptoglobin in chronic liver diseases as a potential biomarker of hepatocellular carcinoma development. Clin Chem Lab Med. 2015;53(1):95–102.

33. Mayampurath A, Song E, Mathur A, Yu C-y, Hammoud Z, Mechref Y, et al. Label-free glycopeptide quantification for biomarker dis-covery in human sera. J Proteome Res. 2014;13(11):4821–32.

34. Mayampurath A, Yu C-Y, Song E, Balan J, Mechref Y, Tang H. Computational framework for identification of intact glycopeptides in complex samples. Anal Chem. 2014;86(4):453–63.

35. Ahn YH, Shin PM, Oh NR, Park GW, Kim H, Yoo JS. A lectin-coupled, targeted proteomic mass spectrometry (MRM MS) plat-form for identification of multiple liver cancer biomarkers in human plasma. J Proteomics. 2012;75(17):5507–15.

36. Ahn YH, Shin PM, Kim Y-S, Oh NR, Ji ES, Kim KH, et al. Quantitative analysis of aberrant protein glycosylation in liver

cancer plasma by AAL-enrichment and MRM mass spectrometry. Analyst. 2013;138(21):6454–62.

37. Ahn YH, Shin PM, Ji ES, Kim H, Yoo JS. A lectin-coupled, mul-tiple reaction monitoring based quantitative analysis of human plas-ma glycoproteins by mass spectrometry. Anal Bioanal Chem. 2012;402(6):2101–12.

38. Lee JY, Kim JY, Park GW, Cheon MH, Kwon K-H, Ahn YH, et al. Targeted mass spectrometric approach for biomarker discovery and validation with nonglycosylated tryptic peptides from N-linked gly-coproteins in human plasma. Mol Cell Proteomics. 2011;10(12): M111.009290.1–13.

39. Link AJ, Eng J, Schieltz DM, Carmack E, Mize GJ, Morris DR, et al. Direct analysis of protein complexes using mass spectrometry. Nat Biotechnol. 1999;17(7):676–82.

40. Kronewitter SR, An HJ, de Leoz ML, Lebrilla CB, Miyamoto S, Leiserowitz GS. The development of retorosynthetic glycan librar-ies to profile and classify the human serum N-linked glycome. Proteomics. 2009;9(11):2986–94.

41. Ozohanics O, Krenyacz J, Ludanyi K, Pollreisz F, Vekey K, Drahos L. GlycoMiner: a new software tool to elucidate glycopeptide com-position. Rapid Commun Mass Spectrom. 2008;22(20):3245–54.

42. Mayampurath AM, Wu Y, Segu ZM, Mechref Y, Tang H. Improving confidence in detection and characterization of protein N-glycosylation sites and microheterogeneity. Rapid Commun Mass Spectrom. 2011;25(14):2007–19.

43. Yuan W, Sanda M, Wu J, Koomen J, Goldman R. Quantitative analysis of immunoglobulin subclasses and subclass specific gly-cosylation by LC-MS-MRM in liver disease. J Proteome. 2015;116:24–33.

44. Takakura D, Harazono A, Hashii N, Kawasaki N. Selective glyco-peptide profiling by acetone enrichment and LC/MS. J Proteomics. 2014;101:17–30.

45. Hortin GL, Sviridov D, Anderson NL. High-abundance polypep-tides of the human plasma proteome comprising the top 4 logs of polypeptide abundance. Clin Chem. 2008;54(10):1608–16.

46. Song E, Mayampurath A, Yu C-Y, Tang H, Mechref Y. Glycoproteomics: identifying the glycosylation of prostate specific antigen at normal and high isoelectric points by LC-MS/MS J. Proteome Res. 2014;13(12):5570–80.

47. Clerc F, Reiding KR, Jansen BC, Kammeijer GSM, Bondt A, Wuhrer M. Human plasma protein N-glycosylation. Glycoconj J. 2015. doi:10.1007/s10719-015-9626-2.

48. Reusch D, Haberger M, Falck D, Peter B, Maier B, Gassner J, et al. Comparison of methods for the analysis of therapeutic immuno-globulin G Fc-glycosylation profiles—Part 2: mass spectrometric methods. mAbs. 2015;7(4):732–42.

49. Gomaa AI, Khan SA, Leen ELS, Waked I, Taylor-Robinson SD. Diagnosis of hepatocellular carcinoma. World J Gastroenterol. 2009;15(11):1301–14.

50. Imre T, Kremmer T, Heberger K, Molnar-Szollosi E, Ludanyi K, Pocsfalvi G, et al. Mass spectrometric and linear discriminant anal-ysis of N-glycans of human serum alpha-1-acid glycoprotein in cancer patients and healthy individuals. J Proteome. 2008;71(2): 186–97.

51. Kondo A, Miyamoto T, Yonekawa O, Giessing AM, Osterlund EC, Jensen ON. Glycopeptide profiling of beta-2glycoprotein I by mass spectrometry reveals attenuated sialylation in patients with antiphospholipid syndrome. J Proteome. 2009;73(1):123–33.

52. Satomi Y, Shimonishi Y, Hase T, Takao T. Site-specific carbohydrate profiling of human transferrin by nano-flow liquid chromatography/electrospray ionization mass spectrometry. Rapid Commun Mass Spectrom. 2004;18(24):2983–8.

53. Arnold JN, Wallis R, Willis AC, Harvey DJ, Royle L, Dwek RA, et al. Interaction of mannan binding lectin with alpha 2 macroglobulin via exposed oligomannose glycans. J Biol Chem. 2006;281(11):6955–63.